Int J Adv Manuf Technol (2017) 91:4191–4201
DOI 10.1007/s00170-017-0076-9

ORIGINAL ARTICLE

A runout measuring method using modeling and simulation cutting force in micro end-milling

Xiubing Jing[1] · **Yanling Tian**[1] · **Yanjie Yuan**[1] · **Fujun Wang**[1]

Received: 12 September 2016 / Accepted: 16 January 2017 / Published online: 10 February 2017

Abstract In the process of micro end-milling, the micro tool axis is not the same line of the spindle axis due to the eccentricity of the tool-holder-spindle assembly, which is called tool runout. Tool runout has significant effects on cutting force variation, which can lead to higher peak forces and uneven tool wear of the cutter. Hence, a runout model must be included in a cutting force modeling to simulate accurate cutting force during micro-milling process. In this paper, the method for modeling and simulation to measure a runout of tool-holder-spindle in micro end-mill was developed. The simulated cutting force with regard to runout was compared with the measured cutting force. It is noted that they had similar variation pattern and closely matched amplitude levels. The result indicated that the effects of tool runout were predominant for the 0.9 mm diameter and at low feed per tooth.

Keyword Micro end-milling · Runout · Laser displacement sensor · Cutting force

1 Introduction

Micro-mechanical machining techniques can produce micro-components with low cost, and the flexibility and efficiency of micro-machining processes using miniature cutting tools allow for the economical fabrication of smaller batch sizes compared with other processes. Micro end-milling was firstly applied in specific fields including electronics, biomedical, and aerospace industries. Recently, the scope of its applications has gradually expanded to meet the increasing demands for micro parts [1]. For micro milling, the ability to automatically generate an optimal process plan can be helpful when using micro milling for micro-product fabrication [2].

In micro-milling, the micro tool axis is not the same line of the holder-spindle axis system due to the eccentricity of the tool-holder-spindle assembly. A runout of tool in holder-spindle system is defined as a tool center deviation with respect to a spindle axis and happens at tool setting [3]. Micro end-milling and conventional end-milling processes are similar as a whole. However, micro tool diameter varies from 0.1 to 1 mm and the chip thickness in micro milling is of the order of 0.5 to 5 μm. Although the variation of tool runout is in the micro scale, it cannot be ignored in micro milling operations compared with macro milling. The tool runout of the micro diameter cutter is more prominent than that of the conventional scale tool, which greatly affects cutting force, increases the maximum cutting force and cutter wear, and affects the dynamic behavior of the cutting process. Hence, investigating effects of the runout on the micro milling plays an important role for improving predicting cutting force and optimal process as long as possible. Force prediction is crucial for the monitoring of the micro-milling process. Cutting force model for micro-milling process have been investigated for machining different workpieces considering various effect factors, such as machining parameters, tool radius, runout, and so on [4–6]. Among all the machining conditions, runout of tool holder-spindle is a major problem in micro milling, as the feed per tooth is relatively small when runout was compared to that in macro milling. To simulate accurate cutting force in micro-milling process, a runout model must be included in a cutting force model.

✉ Xiubing Jing
jingxiuping@tju.edu.cn

[1] Key Laboratory of Equipment Design and Manufacturing Technology, School of Mechanical Engineering, Tianjin University, Tianjin 300072, China

Runout has significant influences on cutting force variation. When measuring cutting force in cutting with multi-cutter tool, we can see that each cutter has a quite different cutting process [7]. The runout measurement was reported by a number of studies. The static runout of the micro-mill is measured by an on-machine camera through an objective lens and a microscope [8]. However, this method cannot measure the runout angle. Afazov measured the static runout using a dial indicator attached to the CNC machine after the cutting tool is clamped onto the spindle [9], and implemented the measurement of the range of runout lengths and angle. Runout also has been tried to predict from measured cutting force waveforms [10], but this method is inappropriate for measuring a run out because it requires an amount of expenses and time for measuring cutting force, moreover, the cutting force signal is distorted in high-speed spindle rotation due to the constraint of the sampling bandwidth of the dynamometer (2~3 kHz). Furthermore, the runout value obtained from this method has some errors because there is the other information in measured cutting force such as tool wear, tool fracture, vibration, etc. Plentiful works demonstrated that the cutter runout in holder-spindle system is an important factor for surface texture and stability prediction in micro-milling process. Therefore, it is very necessary to measure the cutter runout with an accurate and efficient method in practice.

In this paper, a simple, easy to use, and precise method for measuring a static runout of tool-holder-spindle system was developed in micro milling. In this method, the runout of tool-holder-spindle model was developed, a CCD laser displacement sensor was used and the differences of displacement of tool flutes and tool shank were measured. Based on the differences of displacement of tool flutes and tool shank, a runout value of tool holder-spindle can be calculated accurately using the runout model. To verify this method, the simulated cutting force using a calculated runout value was compared with the measured cutting force, and they had similar variation pattern and closely matched amplitude levels.

2 Runout modeling and experimental method

2.1 Runout model

The micro tool center deviation with respect to spindle axis due to the eccentricity of the tool-holder-spindle assembly, a runout of tool holder-spindle is generated in micro-milling process. Runout of the cutting tool is a common problem in the micro-end-milling. A runout can cause the micro tool center deviating from the rotational center and the result makes rotational radiuses of each tool flute to be different each other. A runout of tool holder-spindle system can be defined with a runout length R_0 and a runout angle λ as shown in Fig. 1. Figure 1 shows a general runout model in holder-spindle system for a micro-end-milling, where O' is rotational center of the holder-spindle axis, O is micro tool center. The rotational radius of each tool cutter or each tool flute is dominated by the values of R_0 and λ. From the geometric relationship, the kth tool flute rotational radius can be calculated by Eq. 1 geometrically.

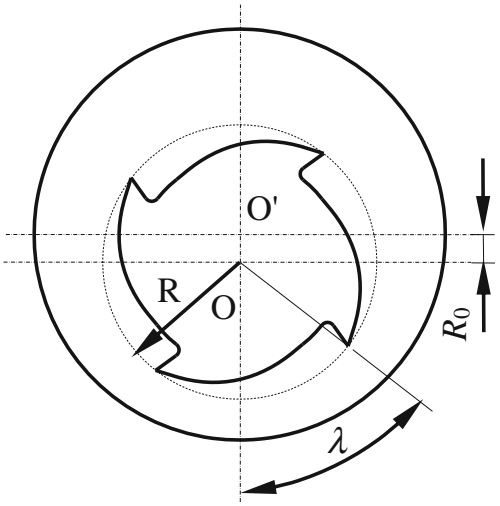

Fig. 1 Definition of runout of tool-holder-spindle system

$$R(k) = \sqrt{R^2 + R_0^2 - 2RR_0\cos\left(\frac{2\pi}{K}(\mathrm{k}-1) - \lambda\right)} \tag{1}$$

where, R is the radius of micro tool, K is the number of flute, k is the kth flute of the tool. The differences between rotational radiuses of adjacent flute can be calculated by Eq. (1). For a micro cutter with K flutes, the K values of $R(1) - R(2)$, $R(2) - R(3)$, …, and $R(K) - R(1)$ can be obtained. Also, $R(K) - R(1)$ can be calculated from the other K-1 values ($R(1) - R(2)$, $R(2) - R(3)$, …, and R (K-1) $- R$ (K) and thus need not to be calculated. From Eq. 1, the K values of differences rotational radiuses can be calculated, the runout R_0 and λ are unknown quantities for each differences rotational radius.

In this paper, it was assumed that the tool flute is distributed perfectly geometrical, and thus the K value of difference between rotational radiuses of tool flutes values is denoted as $DR(1)$, $DR(2)$, …, $DR(\mathrm{K})$ ($DR(1) = (R(1) - R(2)$, $DR(2) = R(2) - R(3)$, … $DR(K) = R(K) - R(1)$). From Fig. 1, the differences of rotational radiuses between the kth flute and the $k + 1$th flute of the tool can be calculated by Eq. 2 geometrically.

$$R(k) - R(k+1) = \sqrt{R^2 + R_0^2 - 2RR_0\cos\left(\frac{2\pi}{K}(k-1) - \lambda\right)} - \sqrt{R^2 + R_0^2 - 2RR_0\cos\left(\frac{2\pi}{K}k - \lambda\right)} \tag{2}$$

For a cutter with K flutes, then differences between rotational radiuses, noted as $DR(1)$, $DR(2)$, $DR(3)$, …. $DR(K)$, can be calculated , which can be described in Eq.3.

$$\begin{aligned} DR(1) &= R(1)-R(2) \\ DR(2) &= R(2)-R(3) \\ DR(K) &= R(K)-R(1) \end{aligned} \tag{3}$$

Based on abovementioned, the diameter of tool with 3 flutes was assumed 0.9 mm, the influence of R_0 and λ on rotational radiuses and the difference between rotational radii can be calculated, as shown in Fig. 2.

It is difficult to measure the rotational radii of tool flute, and calculate R_0 and λ from Eq. 2 and Eq. 3. However, the displacement of tool flute can be directly measured by the laser displacement sensor. When the laser beam is projected onto the rotating center of the spindle, then aligning the laser displacement sensor of CCD to the cutter with K flute, the displacement of the tool flute can be obtained. K peaks (peak (1), peak (2), …, peak (K)) can be obtained when rotating the spindle one revolution. We can define that the measured difference values is $D(1)$, $D(2)$, …, $D(K)$ ($D(1)$ = peak(1) − peak (2), $D(2)$ = peak (2) − peak (3), …, $D(K)$ = peak (K) − peak (1)). When the tool flute is distributed perfectly geometrical and the angles between flutes are correctly equal, the measured difference values ($D(1)$,…, $D(K)$) are same in value, and equal to the differences between rotational radiuses ($DR(1)$,…, $DR(K)$), which can be described in Eq. 4.

$$D(k) = DR(k) = R(k)-R(k+1) \quad (k = 1,\ 2...K) \tag{4}$$

From the K peaks values, the differences between peaks of tool flute can be calculated. Then, the solving was accomplished with a computerized numerical analysis method, the R_0 and λ can be calculated by substituting measured differences between peaks of tool flute to Eq. 2 and Eq. 3.

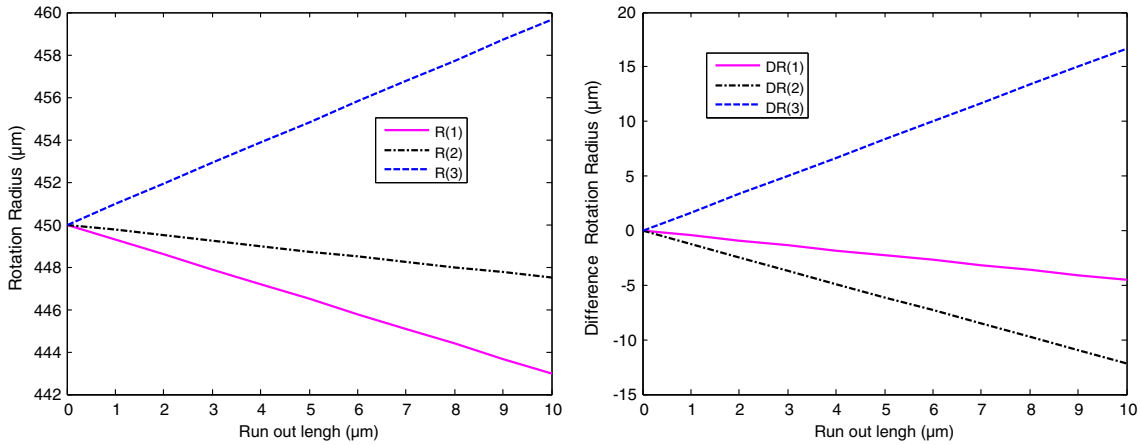

(a) Influence of R_0 on rotational radius and difference rotation radius (λ=45^0)

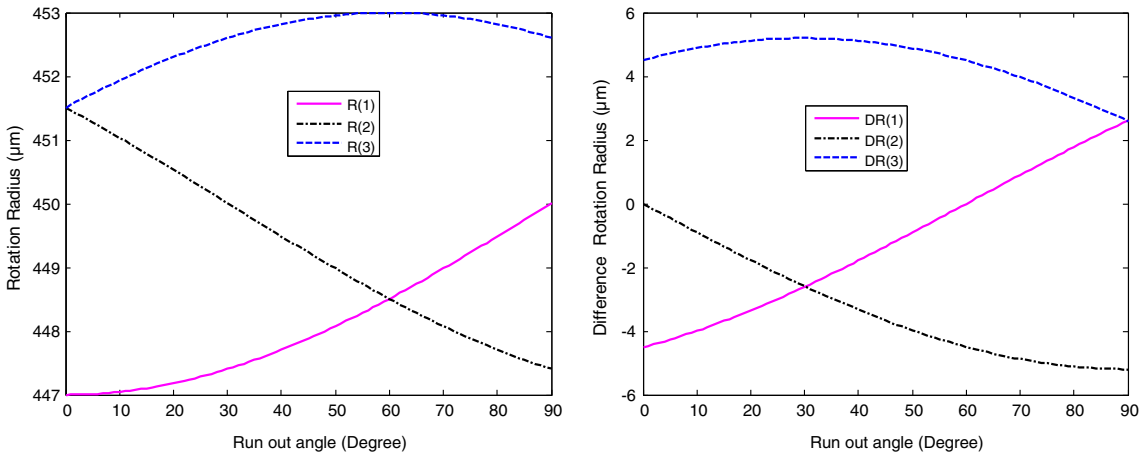

(b) Influence of λ on rotational radius and difference rotation radius (R_0=3)

Fig. 2 Influence of R_0 and λ on rotational radiuses and difference rotational radius. **a** Influence of R_0 on rotational radius and difference rotation radius ($\lambda = 45^0$) and **b** influence of λ on rotational radius and difference rotation radius ($R_0 = 3$)

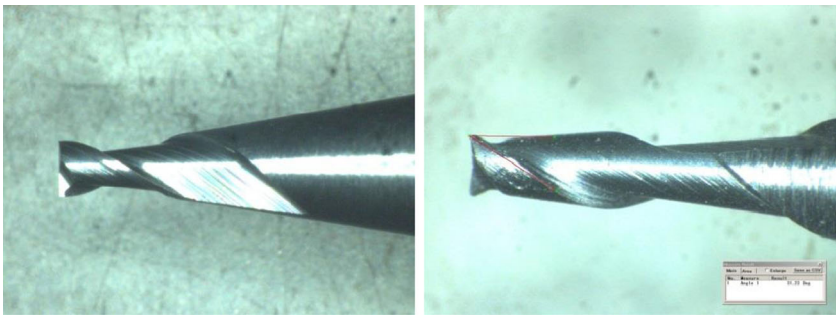

(a) 0.9mm diametercutter (b) 0.6mm diameter cutter

Fig. 3 Microscopic picture of WC micro-mill cutting tool **a** 0.9 mm diameter cutter and **b** 0.6 mm diameter cutter

2.2 Measuring runout by CCD

The micro-cutters in this experiment were uncoated tungsten carbide (WC) flat micro-end-mills of 900 and 600 μm diameter with two flutes. The helix and rake angles were approximately 30° and 10°, respectively. The microscopic picture of the cutter is shown in Fig. 3. The displacement of micro cutter can be measured by using laser displacement.

If the number of flute is two, two peaks (peak (1), peak (2)) can be obtained by aligning laser displacement sensor when rotating the spindle one revolution, and $D(1)$ = peak (1) − peak (2) can be calculated. Substituting $D(1)$ to Eq. 2, the runout R_0 and λ cannot be calculated because there are two unknown quantities in one equation. However, the R_0 can be measured by laser displacement sensor. Aligning the laser displacement sensor to the tool shank, the extreme displacement of the tool shank, the maximum and minimum (R_{max} and R_{min}) can be obtained by using the laser displacement sensor when rotating the spindle one revolution. The value R_0 can be calculated by the maximum and minimum displacement of the tool shank, as following:

$$R_0 = \frac{R_{max} - R_{min}}{2} \tag{5}$$

Substituting R_0 into Eq. 2, λ can be calculated.

The measuring setup for this study is shown in Fig. 4. The setup briefly consists of the revolving spindle and the laser beam sensor supported by a stiffness clamping. The runout can be measured and calculated though four steps.

Step 1: Aligning the laser to the holder-spindle, the center of spindle can be found by iterative method through moving the spindle forward or backward when the minimum displacement can be obtained. The displacement of between laser and spindle is noted as $\triangle x$, when $\triangle x$ is the minimum by moving the spindle, the laser beam is projected onto the rotating center of the spindle, as shown in Fig. 4a.

Step 2: Then, aligning the laser to the tool shank by moving the spindle upward, the extreme displacement of the tool shank the maximum and minimum (R_{max} and R_{min}) can be obtained by using the laser displacement sensor when rotating the spindle one revolution, which is listed in Table.1. The value R_0 can be calculated by the maximum and minimum rotational radius of the tool shank (R_{max} and R_{min}) using Eq. 5.

Step 3: Aligning the laser to the tool tip for measuring the displacement of the tool flute, two peaks (peak (1)

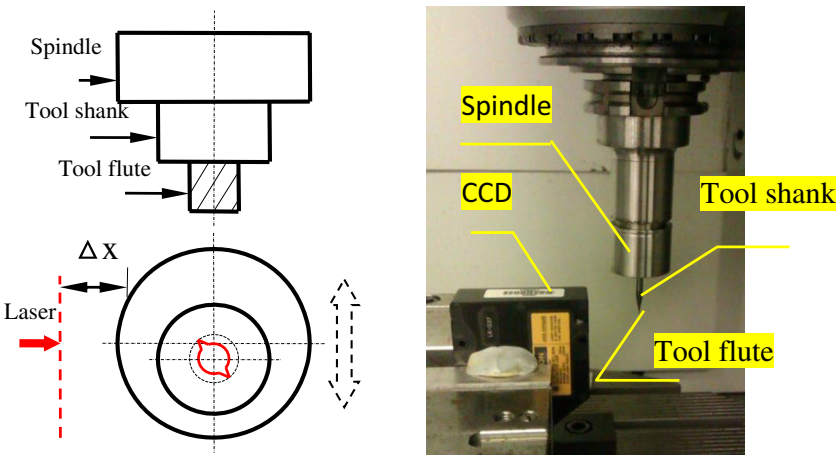

(a) (b)

Fig. 4 The measuring runout setup

Table 1 The measured value and calculated values of runout

Diameter of cutter (μm)	Peak(1) (μm)	Peak(2) (μm)	R_{max} (μm)	R_{min} (μm)	Run out parameters	
					R_0 (μm)	λ (°)
900	379.4	391.2	1941.10	1932.82	5.14	43
600	207.4	208.1	1939.25	1927.15	6.05	2.36

and peak (2)) can be obtained by using the laser displacement sensor when rotating the spindle one revolution, as shown in Fig. 5. We can define that the measured difference values is DR (1) (DR (1) = peak (1) − peak (2)).

Step 4: From Eq. 2, unknown quantities are runout length and runout angle, the differences between rotational radiuses can also be obtained by the peak value of rotational radius of the tool flute, as the following:

$$D(1) = \text{peak}(1) - \text{peak}(2) = R(1) - R(2) \tag{6}$$

Substituting the R_0 into the Eq. 2, λ can be calculated. The measured values and calculated values of runout are shown in Table 1.

3 Experimental validation of the model

3.1 Experiment setup

The Deckel Maho high-speed machining center with computer numerical control (CNC) is utilized to perform the micro end-milling experiments at Lab Advanced Manufacturing, University of New South Wales. The experimental setup for this study is shown in Fig.6. An acoustic emission sensor and accelerometer were used to capture various signals and monitor the milling processes. The accelerometer were attached to the workpiece to measure vibration signal in both X and Y direction. In the experiments for measuring cutting force of micro milling, the two-fluted carbide flat end-mill (as shown in Fig. 3) was used and full immersion slot milling was carried out. The cutting force was measured using a dynamometer (Kistler, 9256C2) with an accuracy of ±0.002 N. The charge signals generated from the force sensor were fed into the charge amplifier (Kistler 5070) which converts the charge signals into voltage signal. The natural frequencies of the X-, Y- and Z- axis of the dynamometer were 4.0, 4.8, and 4.6 kHz, respectively. The forces acting on the tool (X, Y, and Z direction) have been recorded at 10 kHz sampling frequency with a PC-based acquisition system. Micro milling tests at a constant axial depth of cut were conducted. The summary of the experimental conditions is given in Table 2.

The workpiece material chosen for this study is Al. Some mechanical and physical properties of the material are listed in Table 3.

3.2 Cutting force model with runout

To verify the runout model, the cutting force measured from the experiments was compared with the simulated cutting force. In this verification, the basis cutting force model suggested by Armarego was used [11]. Based on the unified mechanics of cutting approach by Armarego, the tangential,

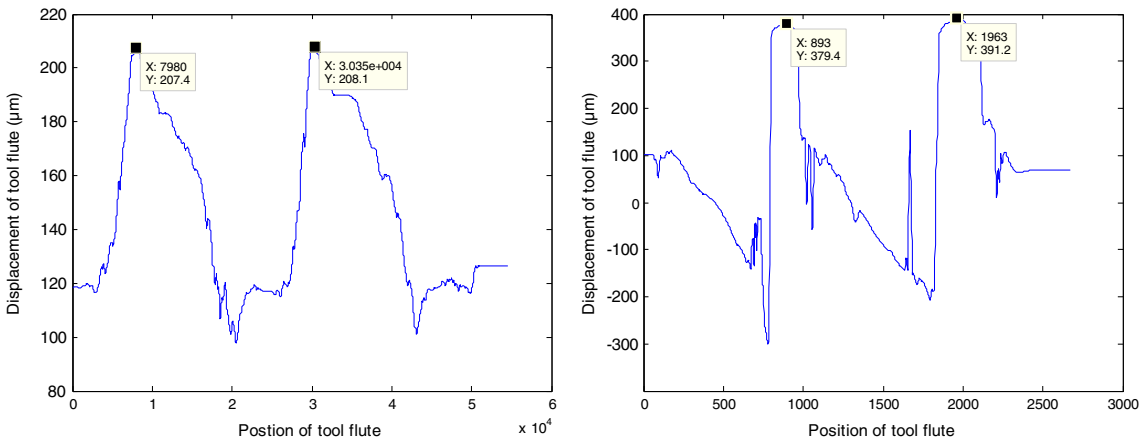

(a) R=300 μm (b) R=450 μm

Fig. 5 Result for displacement of tool flute. **a** R = 300 μm and **b** R = 450 μm

Fig. 6 The experimental setup

feed cutting force coefficients, K_t, K_f, respectively, which account for shear and friction forces in chip formation, are expressed as:

$$K_t = \frac{\tau_s}{\sin\varnothing_n} \frac{\cos(\beta_n - \alpha_n) + \tan^2\eta\sin\beta_n}{\sqrt{\cos^2(\varnothing_n + \beta_n - \alpha_n) + \tan^2\eta\sin^2\beta_n}}$$
$$K_f = \frac{\tau_s}{\sin\varnothing_n\cos i} \frac{\sin(\beta_n - \alpha_n)}{\sqrt{\cos^2(\varnothing_n + \beta_n - \alpha_n) + \tan^2\eta\sin^2\beta_n}} \quad (7)$$

Where τ_s is the shearing stress, ϕ_n and $\beta_n$is the normal shear angle and friction angle, respectively, α_n is the normal rake angle, and η is the chip flow angle which is equal to the oblique angle. Previous research showed that the experimental results in Amarego's model agreed better with the numerical ones, in terms of both error and cutting force values were closest to the experimental ones [17]. Then, the tangential (dF_t) and feed (dF_f) forces cutting force components acting on the tool are considered to be the sum of a term proportional to the area of cut through the cutting coefficients, which can be expressed as Eq. 8:

$$dF_t(\phi) = K_t h(\phi) dz$$
$$dF_f(\phi) = K_f h(\phi) dz \quad (8)$$

where $h(\varphi)$ is the local uncut chip thickness and dz is the depth of cut, φ is the instantaneous immersion angle of the tool. Jing [12] improved the cutting force model proposed by Armarego with a hybrid way, in which the effect of the cutting edge radius, the tool runout and the minimum uncut chip thickness simulated from the FEM has been taken into account.

A micro end-milling process with two flute cutter is shown in Fig. 7. The elemental forces can be integrated along the cutting edge (or edges if a multi-edge tool is considered) and the total cutting forces can be calculated. The elemental forces are resolved into feed and normal directions that can be expressed as:

$$dF_x(\phi) = -dF_t\cos\phi - dF_f\sin\phi$$
$$dF_y(\phi) = dF_t\sin\phi - dF_f\cos\phi \quad (9)$$

To calculate the cutting forces by using Eq. 9, the cutting force coefficients, K_t and K_f, are required. Previous research [13, 14] verified that the cutting force coefficients are variables that are independent of the cutting conditions, such as width of cut, depth of cut, spindle speed, and feedrate. They are determined by the workpiece material, uncut chip thickness, and cutter geometry, such as the helix and the rake angle of the cutter, but not the cutter diameter.

In this model, the cutting forces coefficients for Al calculated by Lee [15] can be used. The proposed instantaneous cutting force coefficients are independent of the end-milling

Table 2 Cutting conditions for micro end-milling

No.	Diameter of cutter (mm)	Axial depth of cut (μm)	Radial depth of cut (mm)	Spindle speed (rpm)	Feedrate (mm/min)	Feed per tooth (μm /tooth)
1	0.9	50	Slotting	10,000	10	0.5
2	0.9	50	Slotting	10,000	30	3
3	0.6	50	Slotting	10,000	10	0.5
4	0.6	50	Slotting	10,000	30	3

Table 3 Physical properties of Al

Elastic modulus (GPa)	70–90
Poisson's ratio	0.33
Density (×1000 kg/m^3)	2.7
Specific heat capacity(J/g-K)	0.896
Thermal conductivity (W/m-K)	180

Table 4 Estimated parameters for the cutting coefficients [15]

k_t [MPa]	k_f [MPa]
A_1 = 7.5080	B_1 = 7.8991
A_2 = 17.7537	B_2 = 18.4467
A_3 = 0.3501	B_3 = 0.3788
A_4 = 81.0565	B_4 = 168.1362

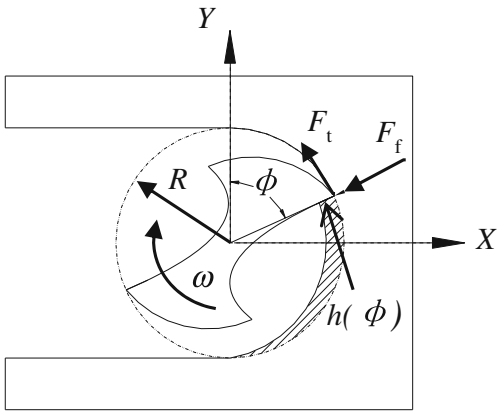

Fig. 7 Micro-milling process with two-fluted micro-end-mill

cutting conditions. These cutting force coefficients, determined from measured cutting forces, reflect the influence of the majority of cutting mechanisms involved in micro end-milling including the minimum chip thickness effect. The relationship between the uncut chip thickness and the acquired normal and frictional cutting force coefficients can be readily fitted in the form of Weibull functions given by Eq. 10, which are nonlinear curve-fitting functions:

$$\begin{aligned} \ln(k_t) &= A_1 - (A_1 - A_2)\exp\left[-(A_4 h)^{A_3}\right] \\ \ln(k_f) &= B_1 - (B_1 - B_2)\exp\left[-(B_4 h)^{B_3}\right] \end{aligned} \tag{10}$$

The parameters of cutting force coefficients in Eq. 10 can be determined from curve-fitting results. The identified parameters are listed in Table 4.

By using these parameters and the estimated uncut chip thickness, the cutting force coefficients are calculated and applied in the cutting force prediction process expressed by Eq. 9. From Eq. 8 and Eq. 9, the instantaneous uncut chip thickness is one of the key parameters for accurately calculation the cutting force in micro end-milling. The instantaneous uncut chip thickness model of conventional milling can be expressed by a sinusoidal function of the feed per tooth based on the assumption of a circular tool path:

$$h(\phi) = f_z \sin(\phi) \tag{11}$$

where f_z is feed per tooth, which cannot precisely describe the instantaneous uncut chip thickness in micro end-milling because the runout has been ignored. In this paper, the instantaneous chip thickness h was evaluated by a mathematical model, the model has taken into account the

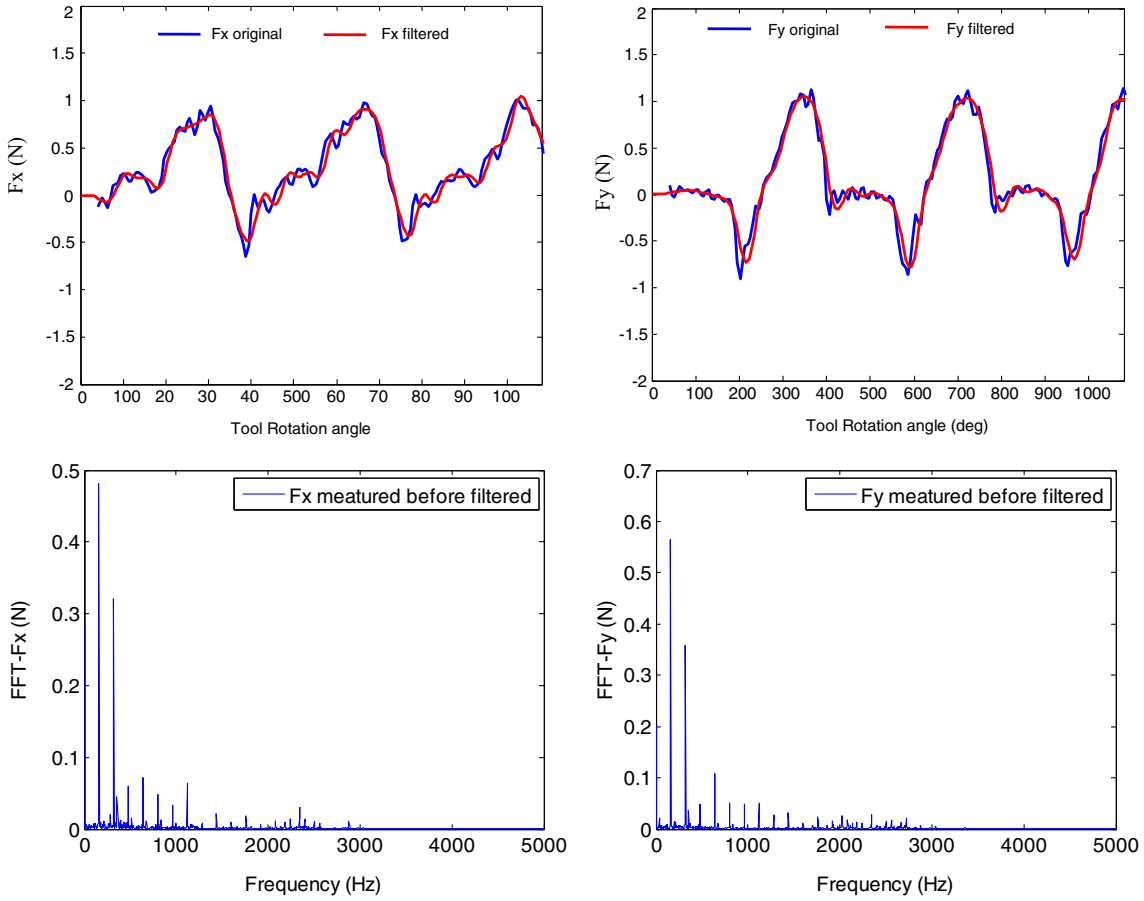

Fig. 8 Experimental cutting force and the frequency spectrums (No.3)

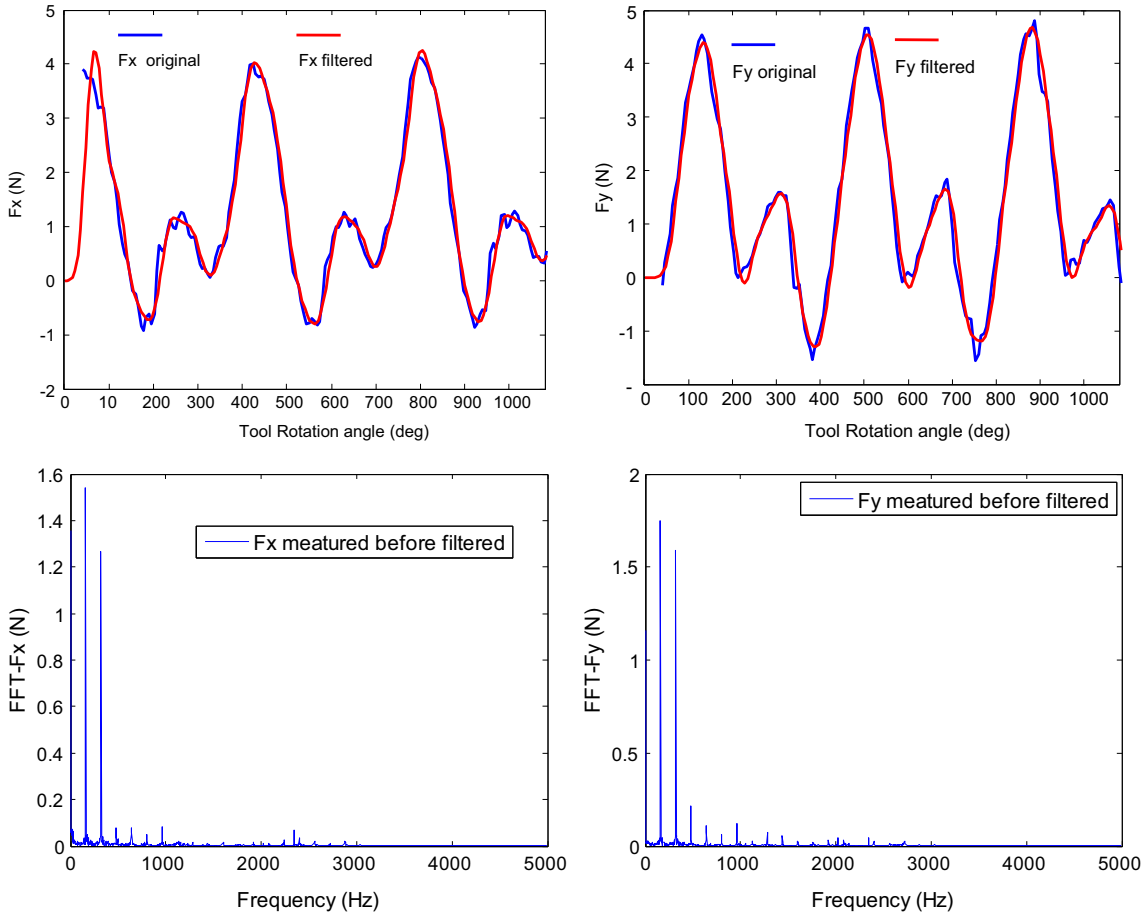

Fig. 9 Experimental cutting force and the frequency spectrums (No.4)

runout effect, angle of rotation, number of flutes, cutting tool radius, feed rate and spindle angular velocity, which can be determined [16] as,

$$h = R + L\sin\left(wt - \frac{2\pi k}{K} + \alpha_0\right) - \sqrt{R^2 - L^2\cos^2\left(wt - \frac{2\pi k}{K} + \alpha_0\right)} \tag{12}$$

where R is radii of micro tool, w is spindle speed, t is the time, L and α_0 is correlated to the run out and feedrate, and can be calculated as suggested in Ref. 16. The runout of tool-holder-spindle for the micro end-mill has been measured; the value has been calculated as mentioned in section 2.2.

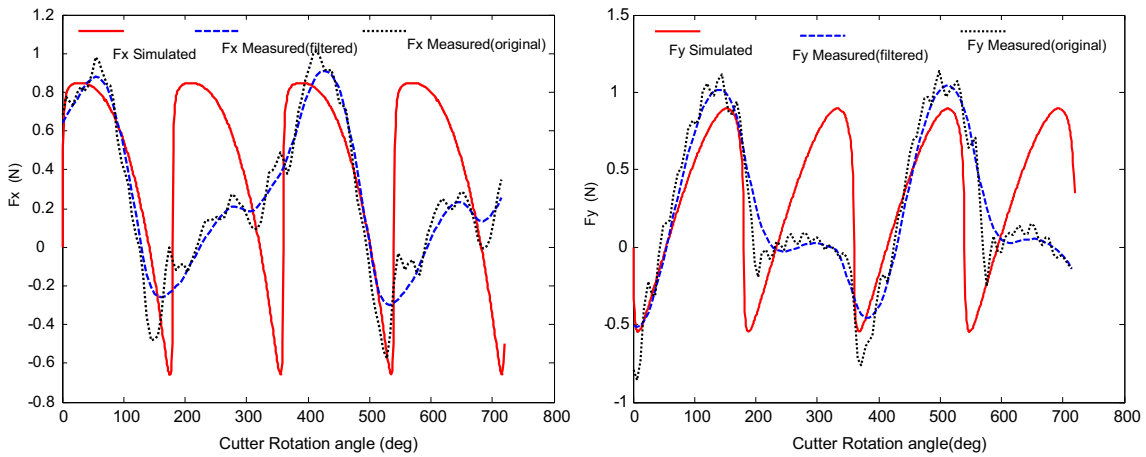

Fig. 10 Predicted cutting force without regard to runout (No.3)

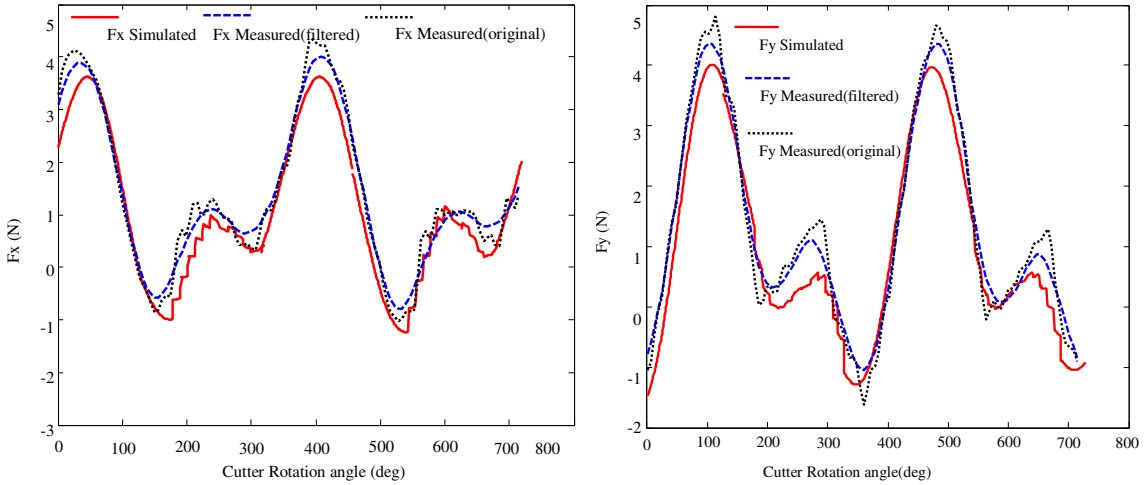

Fig. 11 Comparison of experimental and predicted cutting force (No.4)

3.3 Results of experiments and comparison results

The measured cutting forces are low filtered to compensate the distortion of cutting forces caused by the dynamometer dynamics. Figures 8 and 9 show both the original and low filtered experimental cutting forces in the feed and normal directions during two cutter revolutions, as well as the corresponding frequency spectrum. There are two peaks during one cutter revolution for each tooth, and the force peaks is alternating and varying, that is caused by the cutter runout. From Eq. 12, the instantaneous chip thickness for each tooth is affected by the runout and feed per tooth, which means that the each flute removes different material in the present of tool runout; the peaks of the cutting forces corresponding to extreme instantaneous chip thickness is different for each flute. The high peak in the fast Fourier transform (FFT) of the cutting forces at the frequency corresponding to spindle speed also indicates that tool runout effect plays the important role in micro end-milling. From Fig. 8, it can be observed that when the feed per tooth is 0.5 μm/tooth, there appears to be only one clear force peak within one cutter revolution. However, when the feed per tooth is 3 μm/tooth in Fig. 9, there are two peak forces during one revolution, though the amplitudes of the two peaks are different. This can be explained that the cutter runout significantly affects the cutting force during micro end-milling process. For a two-flute cutter with a runout of tool-holder-spindle, when the feed per tooth is large, both teeth can be engaged in the cutting operation and there are two peak forces in one revolution corresponding to each tooth. However, when the feed per tooth is relatively small, when the runout is higher than the feed per tooth, it is possible that only one tooth is engaged in cutting and the other cuts nothing, so there is one peak force in one revolution.

Based on Eq. 8, 9 and 12, when the runout is zero, the cutting force without regard to run out will be calculated. The predicted cutting force without regard to runout is given in Fig. 10. Both measured and low filtered cutting forces corresponding to no. 3 cutting condition are also illustrated. If not considering runout, the simulated cutting force waves

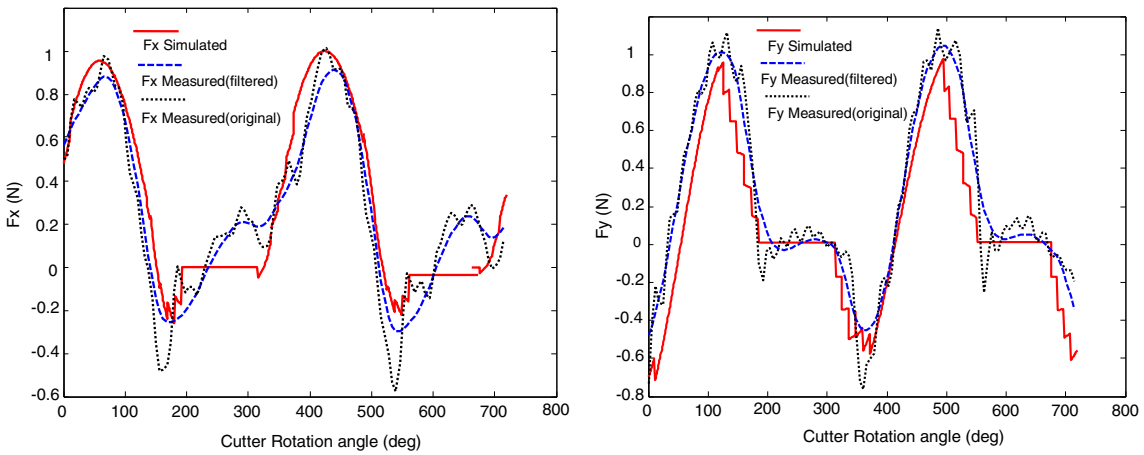

Fig. 12 Comparison of experimental and predicted cutting force (No.3)

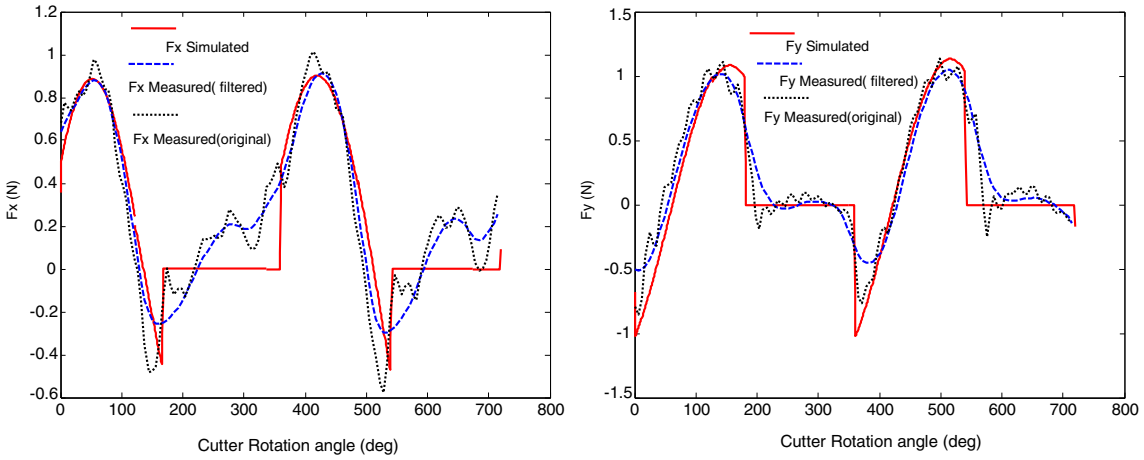

Fig. 13 Comparison of experimental and predicted cutting force (No.1)

always have the same shape and these are different from actual cutting force, as shown in Fig. 10.

Comparisons of the predicted with regard to runout and measured cutting forces corresponding to different cutting conditions are also illustrated in Figs. 11, 12, 13, and 14. The prediction of cutting forces with regard to runout was carried out by using the developed cutting force model in this study. It is shown that both the simulation and measured forces have similar variation pattern and closely matched amplitude levels.

It can be noticed that the forces in the X direction are a slight difference between the measured and the predicted cutting forces at low feed per tooth, while the forces are in very good agreement at high feed per tooth. It can also be seen that there are one peak forces during one revolution with the 0.9 mm diameter cutter in Figs. 13 and 14. Compared to the cutting force predicted and measured corresponding to the 0.6 mm diameter cutter shown in Figs. 11 and 12, it can be noticed that the effect of tooth runout were more profound for the 0.9 mm diameter. This can be explained by the fact that for a fixed spindle speed and feed per tooth, the cutter with a smaller diameter has a lower cutting speed; the cutting speed is higher for the 0.9 mm diameter cutter, which may induce the effect of runout be profound.

4 Conclusions

This paper suggested a new method to measure runout parameters of tool-holder-spindle in micro milling using CCD. The proposed approach is simpler, easy, and precise for measuring runout in micro milling. By using the proposed approach, the runout has been measured. The predicted cutting forces with the runout have been presented. The predicted and the measured forces have been compared in order to verify the measured runout. The differences between displacements of tool flutes, and differences between displacements of tool shank, were measured using a CCD and the runout parameters were calculated. The simulated cutting force with regard to runout was compared with the measured cutting force and they had a

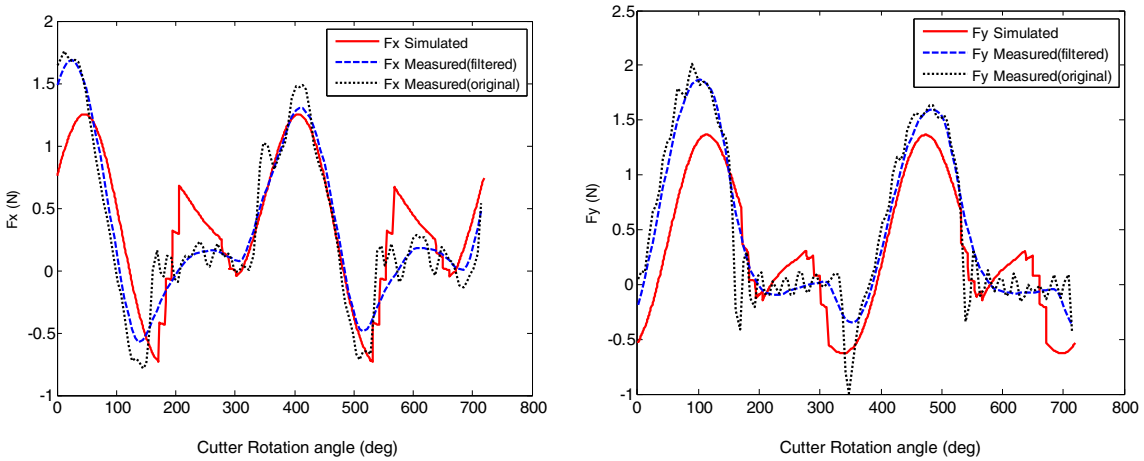

Fig. 14 Comparison of experimental and predicted cutting force (No.2)

good agreement. From the results, we might conclude that runout parameters of R_0 and λ were correctly measured and calculated. The cutter runout significantly affects the cutting force during micro end-milling process. For micro cutters with 0.9 and 0.6 mm diameter, the effect of tooth runout were more profound for the 0.9 mm diameter and at low feed per tooth for both cutters.

Acknowledgements The first author would like to thank the support to this work by the National Foundation of China (Grant No. 51575380). The work was primarily undertaken at UNSW Australia.

References

1. Kang IS, Kim JS, Kim JH, Kang MC, Seo YW (2007) A mechanistic model of cutting force in the micro end milling process. J Mater Process Technol 187-188(12):250–255
2. Ko JH, Cho DW, Ko TJ (2003) Off-line feed rate scheduling for 3D ball-end milling using a mechanistic cutting force model, trans. NAMRI/SME 31:113–120
3. Vogler MP, DeVor RE, Kapoor SG (2003) Microstructure-level force prediction model for micro-milling of multi-phase materials. Journal Manufacturing and Science Engineering 125(2):202–209
4. Kline WA, DeVor RE (1983) The effect of runout on cutting geometry and forces in end milling. International Journal of Machine Tool Design and Research 23(2–3):123–140
5. Vogler MP, DeVor RE, Kapoor SG (2004) On the modelling and analysis of machining performance in micro-endmilling, Part II: Cutting force prediction. Journal Manufacturing and Science Engineering 126(4):695–705
6. Zaman MT, Senthil Kumar A, Rahman M, Sreeram S (2006) A three-dimensional analytical cutting force model for micro end milling operation. Journal Machine Tools & Manufacture 46(3–4):353–366
7. Zheng HQ, Li XP, Wong YS, Nee AYC (1999) Theoretical modeling and simulation of cutting forces in face milling with cutter runout. International Journal Machine Tools & Manufacturing 39(12):2003–2018
8. Xl J, Altintas Y (2012) Prediction of micro-milling forces with finite element method. J Mater Process Technol 212(3):542–553
9. Afazov SM, Ratchev SM, Segal J (2010) Modelling and simulation of micro-milling cutting forces. J Mater Process Technol 210(15): 2154–2162
10. Wang J-JJ (2003) Identification of cutter offset in end milling without a prior knowledge of cutting coefficients. International Journal Machine Tools & Manufacturing 43:687–697
11. Armarego EJA (1998) A generic mechanics of cutting approach to predictive technological performance modelling of the wide spectrum of machining perations, Proceeding of the CIRP International Workshop on Modelling of Machining Operations, Atlanta, Georgia, USA, 95–107
12. Jing XB, Li HZ, Wang J, Tian YL (2014) Modelling the cutting forces in micro-end-milling using a hybrid approach. Journal Advanced Manufacturing Technology 73(9):1647–1656
13. Zhang DL, Mo R, Chang ZY, Sun HB, Li CL (2016) A study of computing accuracy of calibrating cutting force coefficients and run-out parameters in flat-end milling. Journal Advanced Manufacturing Technology 84(1):621–630
14. Ko JH, Cho DW (2005) 3D ball-end milling force model using instantaneous cutting force coefficients. Journal Manufacturing and Science Engineering 127(1):1–12
15. Lee HU, Cho DW, Ehmann KF (2008) A mechanistic model of cutting forces in micro-end-milling with cutting-condition-independent cutting force coefficients. J Manuf Sci Eng 130(3):1–9
16. Li CF, Lai XM, Li HT, Ni J (2007) Modeling of three-dimensional cutting forces in micro-end-milling. J Micromech Microeng 17(4): 671–678
17. Polini W, Prisco U (2003) The estimation of the diameter error in bar turning: a comparison among three cutting force models. Journal Advanced Manufacturing Technology 22(7):465–474